iScience

CellPress
OPEN ACCESS

Article

The role of mitofusin 2 in regulating endothelial cell senescence: Implications for vascular aging

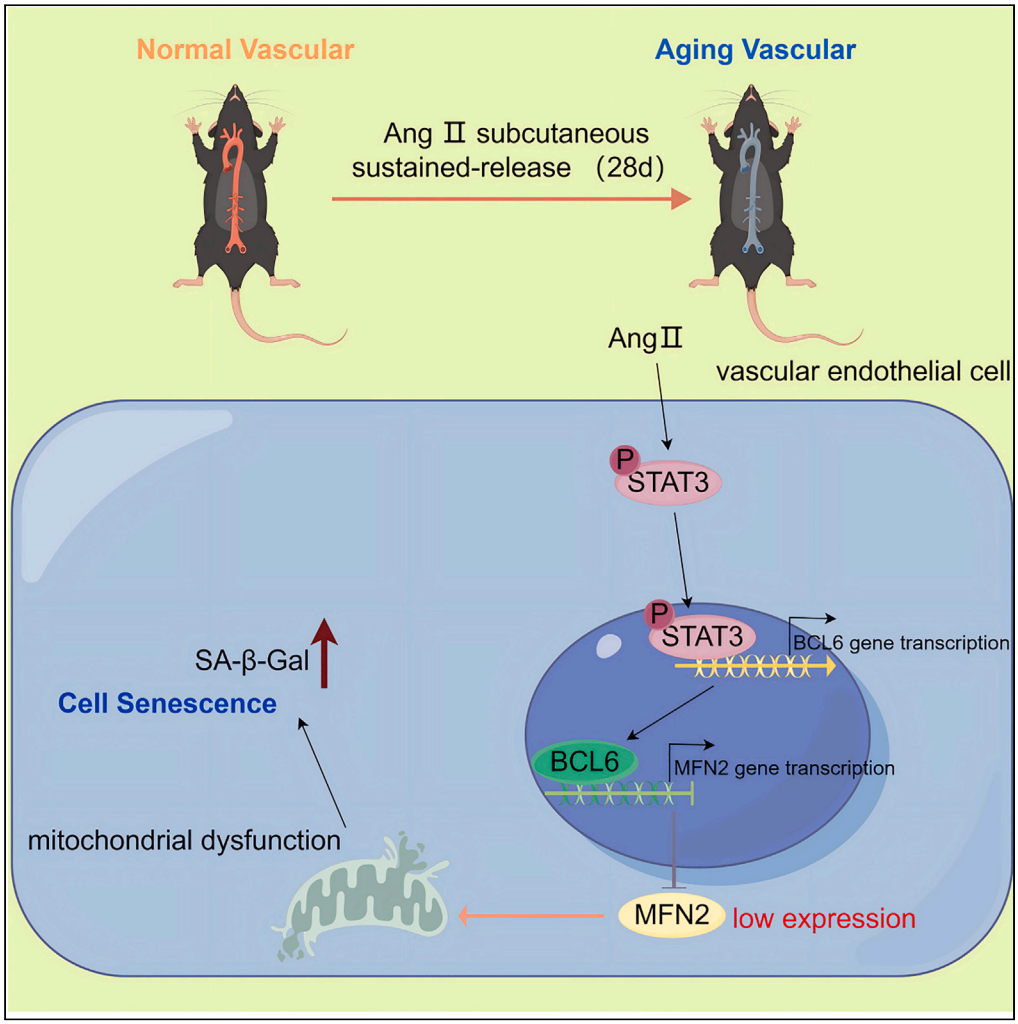

Jiayin Li, Zheming Yang, Haixu Song, ..., Kai Xu, Chenghui Yan, Xiaozeng Wang

wxiaozeng@163.com

Highlights

Angiotensin II activates STAT3, thereby upregulating BCL6 in HUVECs

BCL6, as MFN2 transcriptional repressor, affects vascular aging

MFN2 loss damages mitochondria, causing cell senescence in HUVECs

Li et al., iScience 27, 110809
September 20, 2024
https://doi.org/10.1016/j.isci.2024.110809

iScience

CellPress
OPEN ACCESS

Article

The role of mitofusin 2 in regulating endothelial cell senescence: Implications for vascular aging

Jiayin Li,[1,2] Zheming Yang,[1,2] Haixu Song,[2] Lin Yang,[2] Kun Na,[2] Zhu Mei,[1,2] Shuli Zhang,[1,2] Jing Liu,[2] Kai Xu,[2] Chenghui Yan,[2] and Xiaozeng Wang[2,3,*]

SUMMARY

Endothelial cell dysfunction contributes to age-related vascular diseases. Analyzing public databases and mouse tissues, we found decreased MFN2 expression in senescent endothelial cells and angiotensin II-treated mouse aortas. In human endothelial cells, Ang II reduced MFN2 expression while increasing senescence markers P21 and P53. *siMFN2* treatment worsened Ang II-induced senescence, while MFN2 overexpression alleviated it. *siMFN2* or Ang II treatment caused mitochondrial dysfunction and morphological abnormalities, including increased ROS production and reduced respiration, mitigated by *ovMFN2* treatment. Further study revealed that BCL6, a negative regulator of MFN2, significantly contributes to Ang II-induced endothelial senescence. *In vivo*, Ang II infusion decreased MFN2 expression and increased BCL6, P21, and P53 expression in vascular endothelial cells. The *shMfn2*+Ang II group showed elevated senescence markers in vascular tissues. These findings highlight MFN2's regulatory role in endothelial cell senescence, emphasizing its importance in maintaining endothelial homeostasis and preventing age-related vascular diseases.

INTRODUCTION

Aging is a complex biological process characterized by a progressive decline in the functional capacity of tissues and organs, leading to an increased susceptibility to age-related diseases.[1,2] The vascular system, which plays a crucial role in maintaining tissue homeostasis and organ function, undergoes significant changes with age.[3,4] One of the key contributors to vascular aging is the dysfunction of endothelial cells,[5] which line the inner surface of blood vessels and regulate vascular tone and homeostasis.

Endothelial cell senescence, a state of irreversible growth arrest, is considered a hallmark of vascular aging.[6] It is associated with impaired endothelial function, increased oxidative stress, chronic low-grade inflammation, and altered angiogenic potential.[7,8] Various factors, including reactive oxygen species (ROS), DNA damage, telomere attrition, and chronic exposure to cardiovascular risk factors, contribute to endothelial cell senescence.[9–11] Understanding the molecular mechanisms underlying endothelial cell senescence is crucial for developing strategies to delay or prevent age-related vascular diseases.

Some studies have identified the Mitofusin 2 (MFN2) protein as a key regulator of mitochondrial dynamics and function, with emerging evidence suggesting its involvement in cellular senescence.[12–14] MFN2 is a transmembrane GTPase protein localized to the outer mitochondrial membrane and is responsible for maintaining mitochondrial fusion and fission balance.[15] Dysregulation of MFN2 has been implicated in several age-related diseases, including neurodegenerative disorders, metabolic syndrome, and cardiovascular diseases.[16–18]

The renin-angiotensin system (RAS), a major hormonal regulator of blood pressure and fluid balance, has also been implicated in vascular aging.[19] Angiotensin II (Ang II), a key effector peptide of the RAS, exerts its biological effects by binding to angiotensin receptors on endothelial cells, resulting in vasoconstriction, inflammation, and oxidative stress.[20,21] Chronic exposure to Ang II has been shown to promote endothelial cell senescence and contribute to vascular dysfunction.[22]

Although the role of MFN2 in mitochondrial dynamics and its implications in aging-related diseases have been extensively studied, its involvement in Ang II-induced endothelial cell senescence remains poorly understood. This gap in knowledge presents an exciting opportunity to investigate the potential role of MFN2 in regulating Ang II-induced endothelial cell senescence and its impact on vascular aging.

In this study, we aim to elucidate the molecular mechanisms underlying MFN2-mediated regulation of endothelial cell senescence in response to Ang II stimulation. We hypothesize that MFN2 plays a critical role in maintaining mitochondrial function and morphology in endothelial cells, and its dysregulation contributes to Ang II-induced endothelial cell senescence. By understanding the specific molecular pathways involved, we hope to identify potential therapeutic targets for delaying or preventing age-related vascular diseases.

[1]College of Medicine and Biological Information Engineering, Northeastern University, Shenyang, Liaoning 110167, China
[2]State Key Laboratory of Frigid Zone Cardiovascular Diseases, Cardiovascular Research Institute and Department of Cardiology, General Hospital of Northern Theater Command, Shenyang 110016, China
[3]Lead contact
*Correspondence: wxiaozeng@163.com
https://doi.org/10.1016/j.isci.2024.110809

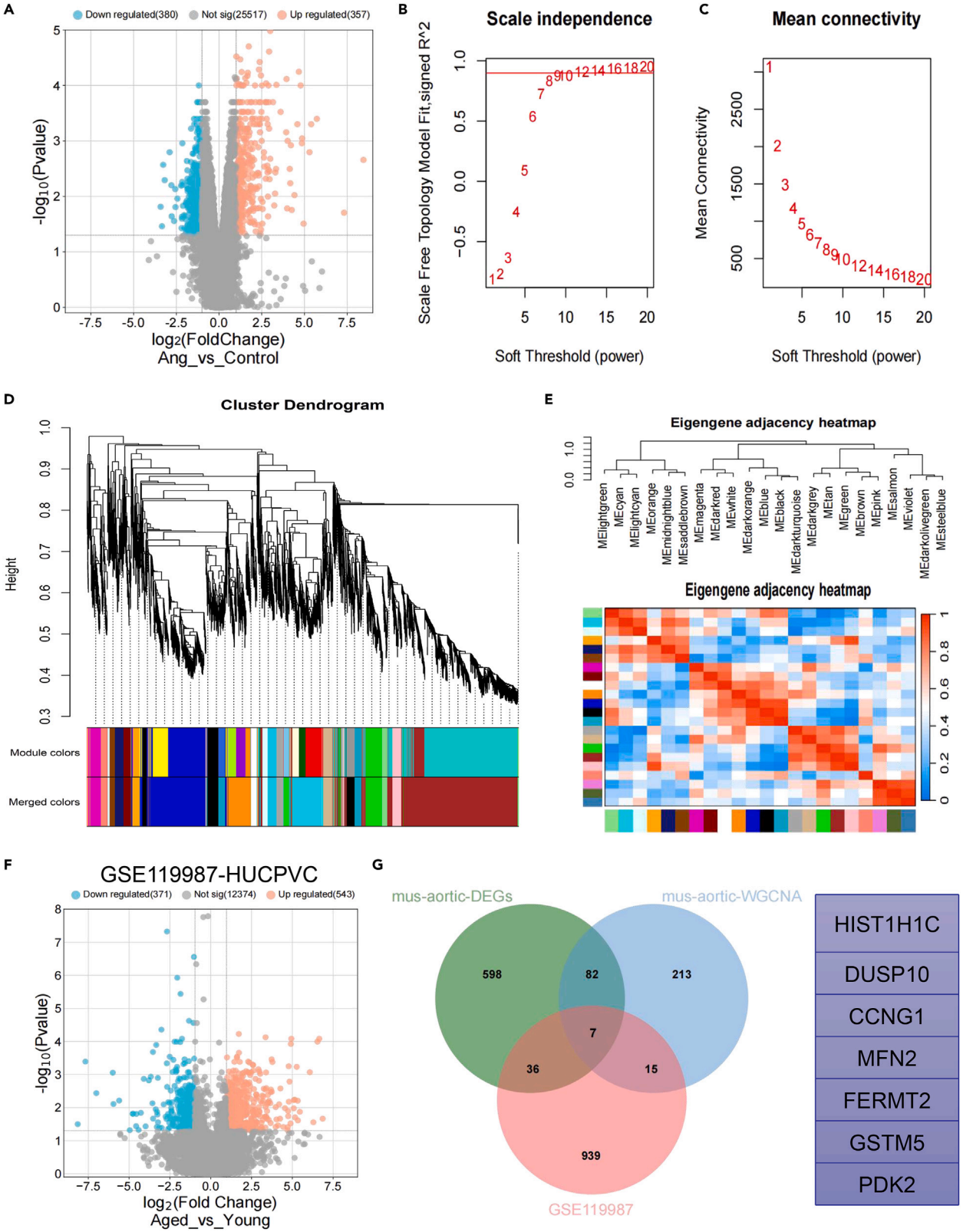
A
Down regulated(380)
Not sig(25517)
Up regulated(357)
-log10(Pvalue)
log2(FoldChange)
Ang_vs_Control
B
Scale independence
Scale Free Topology Model Fit,signed R^2
Soft Threshold (power)
C
Mean connectivity
Mean Connectivity
Soft Threshold (power)
D
Cluster Dendrogram
Height
Module colors
Merged colors
E
Eigengene adjacency heatmap
MElightgreen
MEcyan
MElightcyan
MEorange
MEmidnightblue
MEsaddlebrown
MEmagenta
MEdarkred
MEwhite
MEdarkorange
MEblue
MEblack
MEdarkturquoise
MEdarkgrey
MElan
MEgreen
MEbrown
MEpink
MEsalmon
MEviolet
MEdarkolivegreen
MEsteelblue
Eigengene adjacency heatmap
F
GSE119987-HUCPVC
Down regulated(371)
Not sig(12374)
Up regulated(543)
-log10(Pvalue)
log2(Fold Change)
Aged_vs_Young
G
mus-aortic-DEGs
mus-aortic-WGCNA
GSE119987
598
82
213
7
36
15
939
HIST1H1C
DUSP10
CCNG1
MFN2
FERMT2
GSTM5
PDK2

Figure 1. Screening of major aging-related differential genes

(A) Volcano plot of differential gene expression in mouse aortic microarray data after AngII infusion, blue represents down-regulation, and red represents up-regulation. Cutoff: |log2(FC)| > 1 and $p < 0.05$.

(B and C) The scale independence and the mean connectivity to identify the soft threshold with the best performance.

(D) Hierarchical cluster dendrogram and color-coding of gene co-expression modules.

(E) Heatmap of eigengene adjacency.

(F) Volcano plot and gene list of differential gene expression in GEO: GSE119987 dataset, blue represents down-regulation and red represents up-regulation. Cutoff: |log2(FC)| > 1 and $p < 0.05$.

(G) The Venn diagram of genes among mus-aortic-DEGs, mus-aortic-WGCNA, and GEO: GSE119987-DEGs.

RESULTS

Mitofusin 2 is expressed at low levels in various types of senescent vessel-associated cells

To identify key regulatory genes associated with aging in mouse aortic tissues, we performed differential analysis of microarray data from mouse aortic tissues to identify differentially expressed genes (DEGs) (Figure 1A). We used weighted gene co-expression network analysis (WGCNA) to construct a co-expression network in mouse aortic tissue and selected the main green modules for subsequent analysis (Figures 1B–1E). Subsequently, we analyzed the HUCPVCs database GEO: GSE119987 to identify DEGs during replicative senescence, which resulted in the identification of DEGs (Figure 1F). By intersecting the gene sets from these different analyses, we obtained 7 genes of interest (Figure 1G). To validate the expression consistency of these 7 genes across the two datasets, we extracted their expression profiles and found that only two genes, MFN2 and FERMT2, exhibited significantly decreased expression in both datasets (Figures 2A and 2B).

Given the importance of mitochondrial damage and reactive oxygen species (ROS) production in aging processes, and recognizing that MFN2 is a crucial mitochondrial fusion protein, we focused on the MFN2 gene and further investigated its expression in other senescent vessel-related cells. We observed significant downregulation of MFN2 in aged mouse vascular aortic tissues (Figure 2C), as well as in IR-induced senescent HMVMCs (Figure 2D) and HUVECs (Figure 2E). These findings suggest that MFN2 is consistently and markedly underexpressed in senescent vessel-related cells affected by various factors.

Mitofusin 2 is involved in the regulation of angiotensin II -induced endothelial cell senescence

To examine the expression changes of MFN2 in an endothelial cell senescence model, HUVECs were stimulated with various concentrations of Ang II for 24 to 36 h. Results showed that the protein and mRNA levels of MFN2 initially increased and then decreased with the duration of stimulation. After 36 h of Ang II stimulation at a concentration of 10 μM, the expression of senescence-related genes P21 and P53 significantly increased (Figures S1A–S1C).

Next, we performed Beta-galactosidase (β-Gal) staining and Ki67 immunofluorescence staining on HUVECs stimulated with Ang II (10 μM, 36 h) to assess cell senescence and proliferation. We observed a significant decrease in cell proliferation and an increase in the number of senescent cells after Ang II stimulation (Figures 3A–3C). At the protein level, we found that MFN2 expression was downregulated, while P21 and P53 expression were upregulated following Ang II stimulation (Figures 3D and 3E). These findings suggest that the reduction in MFN2 may contribute to Ang II-induced endothelial cell senescence.

To further establish the role of MFN2 in Ang II-induced endothelial cell aging, we separately introduced *siMFN2* and *ovMFN2* while administering Ang II stimulation to assess changes in cell aging and proliferation. The efficiency of *siMFN2* and *ovMFN2* treatments is shown in Figures S2B and S2C β-Gal and Ki67 staining demonstrated that pure *siMFN2* treatment induced aging. Compared to the Ang II group, *siMFN2*+Ang II treatment resulted in reduced cell proliferation and aggravated cell senescence, while *ovMFN2*+Ang II treatment attenuated Ang II-induced cell senescence and increased cell proliferation (Figures 4A–4D). At the protein level, *siMFN2* treatment significantly increased the levels of P21 and P53, and these changes were further accentuated by Ang II (Figures 4E and 4F). Conversely, *ovMFN2* significantly reduced the Ang II-induced increase in P21 and P53 protein levels, thereby alleviating cell senescence (Figures 4G and 4H).

Reduction of mitofusin 2 leads to cellular senescence by impacting mitochondrial morphology and function

It is widely recognized that MFN2 is a critical mitochondrial fusion protein, and mitochondria play a crucial role in cellular senescence. To investigate the mechanisms underlying cellular senescence resulting from MFN2 depletion, we examined mitochondrial morphology and function in endothelial cells. MitoTracker (Green) and MitoSOX (Red) staining revealed that after Ang II stimulation or MFN2 silencing, mitochondria exhibited significant fragmentation and increased ROS production. The fluorescence co-localization was markedly enhanced compared to normal cells. In comparison to the Ang II group, the *siMFN2*+Ang II group exhibited exacerbated mitochondrial morphological damage and elevated ROS levels. Conversely, the *ovMFN2*+Ang II group displayed reduced co-localization of the two fluorescence sources, promoting mitochondrial fusion and reducing ROS production, thus mitigating mitochondrial damage (Figures 5A and 5B).

Furthermore, mitochondrial respiration was assessed using a Seahorse bioanalyzer to evaluate changes in mitochondrial function across the six groups. The oxygen consumption rate (OCR) of mitochondria in each group was analyzed (Figure 5C). The results revealed that basal respiration (Figure 5D), maximal respiration (Figure 5E), ATP production (Figure 5F), and spare respiratory capacity (Figure 5G) of mitochondria were significantly decreased following *siMFN2* treatment and Ang II stimulation compared to the normal group. Similar to the findings mentioned above, the *siMFN2*+Ang II group demonstrated further impairment of these indicators, while the *ovMFN2*+Ang II group exhibited alleviation of these issues. These findings indicate that MFN2 may influence endothelial cell aging by modulating mitochondrial morphology and function.

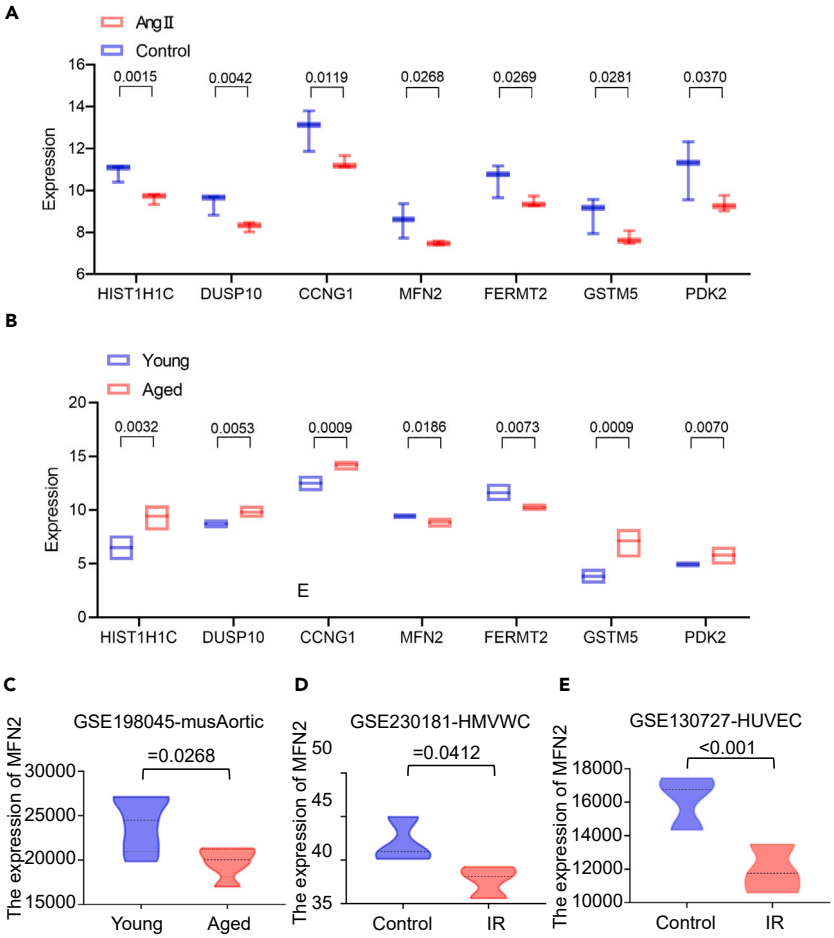

Figure 2. MFN2 plays a key role in aortic and vascular endothelial cell senescence

(A) Expression of 7 genes in aortae of mice after Ang II infusion. Each bar represents the mean ± SD.

(B) Expression of 7 genes in GEO: GSE119987. Each bar represents the mean ± SD.

(C) MFN2 was significantly downregulated in the GEO: GSE198045 dataset. Each bar represents the mean ± SD.

(D) MFN2 was significantly downregulated in the GEO: GSE230181 dataset. Each bar represents the mean ± SD.

(E) MFN2 was significantly downregulated in the GEO: GSE130727 dataset. Each bar represents the mean ± SD.

Angiotensin II regulates mitofusin 2-induced endothelial cell senescence by upregulating the expression of B-cell lymphoma 6

To elucidate the mechanism underlying the regulation of MFN2-induced endothelial cell senescence by Ang II, we predicted transcription factors upstream of the MFN2 promoter region in humans and mice using JASPAR: https://jaspar.elixir.no/. We then intersected the differentially expressed genes in the GEO: GSE130727 dataset and a mouse aortic tissue microarray to generate a Venn diagram (Figure 6A). BCL6 emerged as a potential major transcription factor regulating MFN2 during cellular senescence, and the binding sites of BCL6 to the MFN2 promoter region are depicted in Figure 6B.

To determine if BCL6 is the primary upstream transcription factor of MFN2 in Ang II-induced endothelial cell senescence, we examined the protein expression of BCL6 in Ang II-induced endothelial cells. The results demonstrated that BCL6 expression significantly increased following Ang II stimulation (Figure 6C). Dual-luciferase reporter gene assays revealed that BCL6 suppressed the activity of the MFN2 promoter region. Additionally, the mutation of the BCL6 binding site in the MFN2 promoter region led to a significant reduction in the activity of the MFN2 promoter (Figure 6D).

Subsequently, we investigated whether changes in BCL6 expression could affect endothelial cell senescence by evaluating the protein levels of P21 and P53 using *siBCL6* and *ovBCL6*, respectively. The efficiencies of *siBCL6* and *ovBCL6* treatments are presented in Figures S2E and S2F. Western blot analysis and quantitative results demonstrated that *siBCL6* treatment significantly upregulated MFN2 expression while downregulating P21 and P53 expression. Conversely, *ovBCL6* treatment downregulated MFN2 expression and upregulated P21 and P53 expression (Figures 6E–6H). Moreover, *siBCL6* treatment significantly mitigated the increase in P53 and P21 expression induced by *siMFN2*, thereby attenuating endothelial cell senescence (Figures 7A and 7C). Similarly, *ovMFN2* treatment significantly ameliorated the

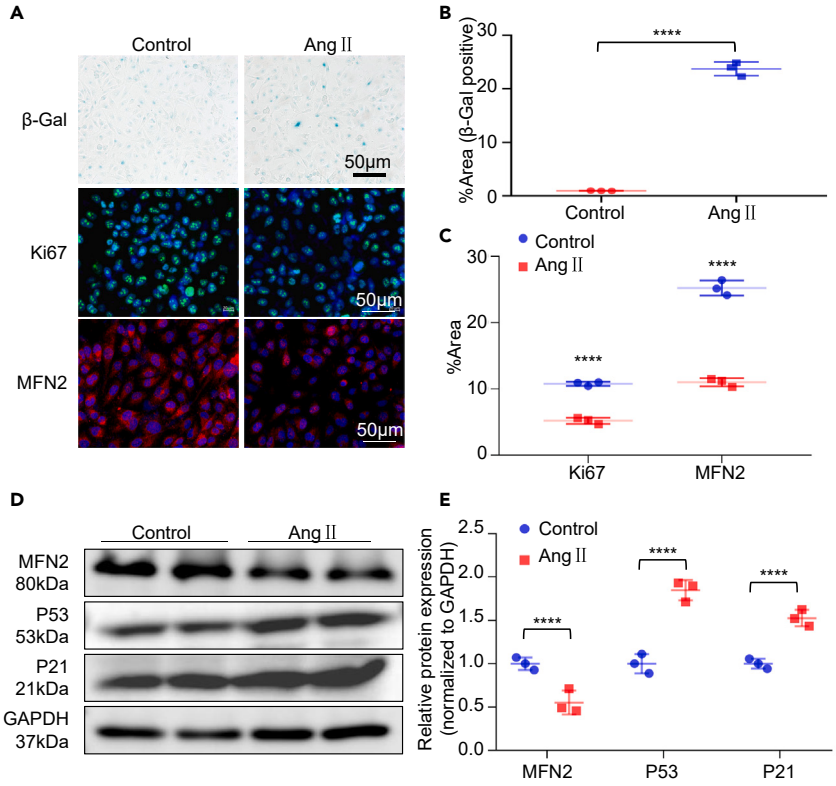

Figure 3. MFN2 is lowly expressed in AngII-induced senescent HUVECs

(A) HUVECs were stimulated with angiotensin 2 (10 μM) for 36 h, then β-Gal staining and immunofluorescence staining, and quantification of Ki67 and MFN2 were performed.

(B and C) Quantitative analysis of staining. Each bar represents the mean ± SD for triplicate experiments (****$p < 0.0001$).

(D) The protein expression and (E) quantification of senescence-related marker proteins were detected after HUVECs were stimulated with Ang II. Each bar represents the mean ± SD for triplicate experiments. Mean data are normalized to GAPDH (****$p < 0.0001$).

decreased expression of MFN2 and the increased expression of P53 and P21 induced by *ovBCL6*, consequently alleviating endothelial cell senescence caused by BCL6 overexpression through the upregulation of MFN2 expression (Figures 7B and 7D). These findings suggest that Ang II influences endothelial cell senescence by regulating the BCL6/MFN2 axis. In order to verify the BCL6 role in the age dependence of MFN2 reduction process, we further Ang II subcutaneous sustained-release 0 days, 3 days, 7 days and 28 days mice aorta tissue paraffin section BCL6 and immunofluorescence staining of MFN2, found that MFN2 and BCL6 high expression in aortic endothelial cells, The expression of BCL6 increased, while the expression of MFN2 decreased with the increasing AngII infusion time (Figure S3A).

Knockdown of mitofusin 2 exacerbated angiotensin II-induced vascular endothelial cell senescence in mice

To verified that MFN2 deficiency accelerates endothelial cell senescence *in vivo*, ApoE$^{-/-}$ mice were injected with AAV-*shMfn2* adeno-associated virus (*shMfn2*) via the tail vein, followed by subcutaneous sustained release of Ang II for 28 days. Since endothelial cells are flat epithelial cells that line the inner surface of blood vessels and lymphatic vessels, aortic tissues were collected from sacrificed mice for further experiments. The efficacy of MFN2 knockdown was evaluated, and the mRNA level of Mfn2 was significantly reduced in the vascular tissues of *shMfn2* group mice (Figure 8A). CD31 and MFN2 co-immunofluorescence staining of mouse aortic tissue sections revealed that MFN2 expression in endothelial cells decreased after Ang II stimulation, and the expression of MFN2 was even lower in the *shMfn2*+Ang II group (Figure 8B). The results of the ROS assay showed that compared with the control group, the generation of ROS in the aorta significantly increased after Ang II infusion, and mitochondria released more ROS, leading to tissue damage following *shMfn2* treatment (Figures 8C and 8D). Subsequently, β-Gal staining was performed in vascular tissue, which revealed that the *shNC*+Ang II group had a significantly increased β-Gal positive area compared to the *shNC* group. Furthermore, the *shMfn2*+Ang II group exhibited an even more significant β-Gal positive area compared to the *shNC*+Ang II group (Figures 8E and 8F). These findings indicated that *shMfn2* could exacerbate Ang II-induced vascular senescence in mice.

Meanwhile, BCL6, P21, and P53 were up-regulated, while MFN2 was down-regulated in the vascular tissues of Ang II-treated mice (Figures 9A and 9B). In comparison to the shNC+Ang II group, the expression of MFN2 in the vascular tissues of the *shMfn2*+Ang II group

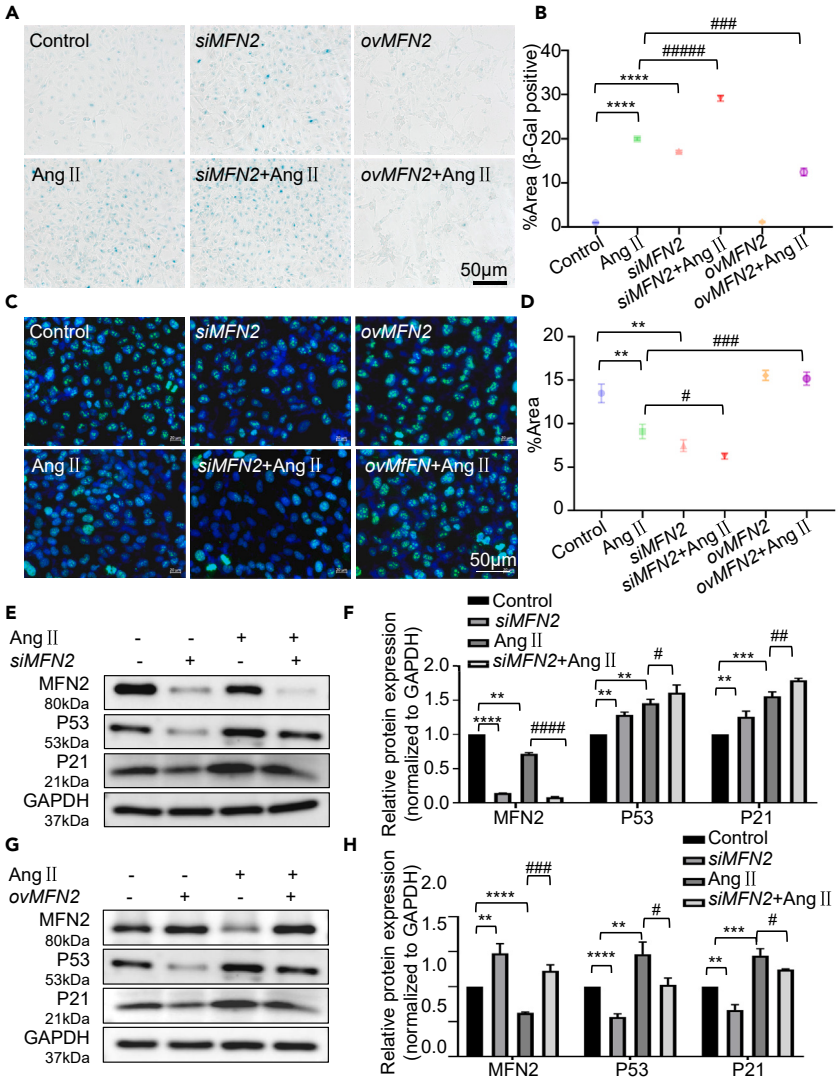

Figure 4. MFN2 overexpression can increase endothelial cell proliferation and reduce senescence

(A) HUVECs were stimulated with Ang II after *siMFN2*/*ovMFN2*. After 36 h, β-Gal staining was performed, (B) and the staining was quantified.

(C) HUVECs were stimulated with Ang II after *siMFN2*/*ovMFN2*. Immunofluorescence staining of Ki67 was performed, (D) and the staining was quantified.

(E) To investigate the effect of *siMFN2* followed by Ang II stimulation on the protein expression and (F) quantification of P53 and P21 proteins. Mean data are normalized to GAPDH.

(G) Effects of *ovMFN2* followed by Ang II stimulation on P53 and P21 protein expression and (H) quantification. Mean data are normalized to GAPDH. In (B, D, F, and H), each bar represents the mean ± SD for triplicate experiments (**$p < 0.01$, ***$p < 0.001$, ****$p < 0.0001$; #$p < 0.05$, ##$p < 0.01$, ###$p < 0.001$, ####$p < 0.0001$).

was significantly decreased, whereas the expressions of P21 and P53 were significantly increased (Figures 9C and 9D). These results suggested that loss of MFN2 aggravates Ang II-induced vascular senescence.

Angiotensin II by activating the phosphorylation of STAT3 expression to activate the B-cell lymphoma 6 expression to promote vascular endothelial cell senescence

To explore how Ang II increases the molecular mechanism of inducing BCL6 expression, we through the trust website (Trust: https://www.grnpedia.org/trrust/) search the BCL6 upstream of the transcription factor, FOSL2, FOXO3, FOXO4, JUND, and STAT3 were found to activate BCL6 expression. Among these molecules, STAT3 is a pro-aging transcription factor closely related to aging. Therefore, we examined the expression and phosphorylation of STAT3 in HUVECs after AngII stimulation. We found that p-STAT3 was highly expressed after AngII stimulation (Figures 10A and 10B). Likewise, we predict the BCL6 promoter region of STAT3 binding sites, as shown in Figure 10C. To validate the role of STAT3 in AngII-induced endothelial cell senescence, we treated HUVECs with p-STAT3 inhibitor (S31-201) in the presence of AngII.

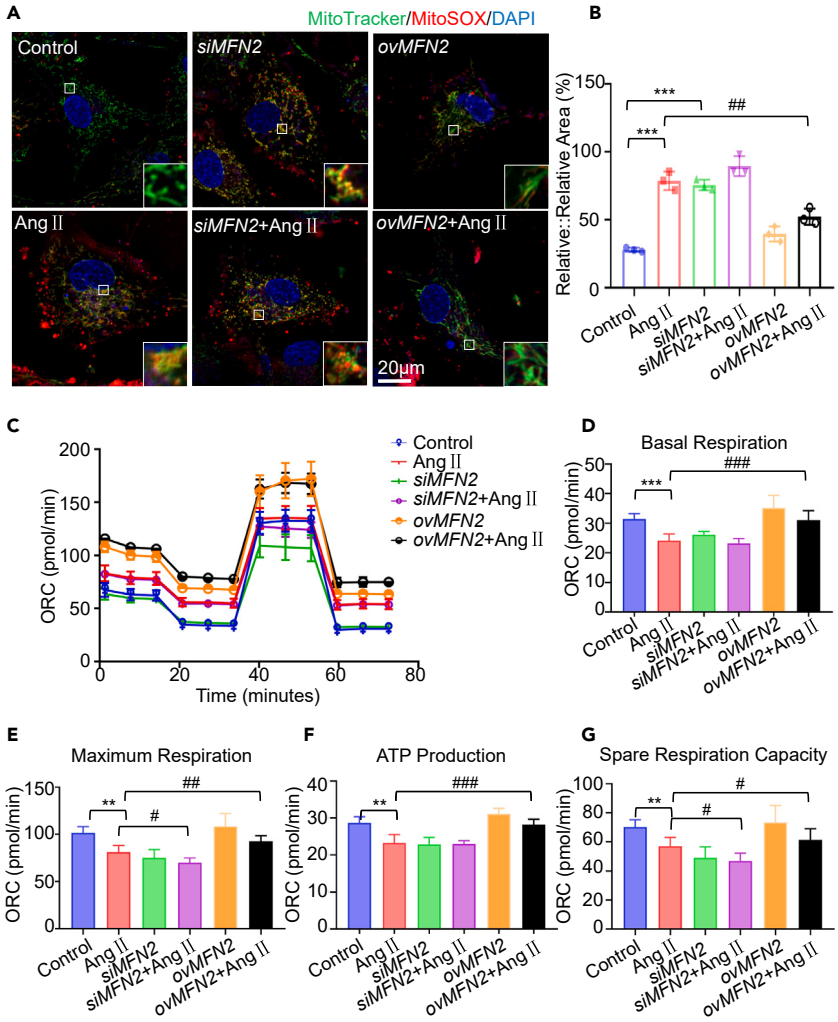

Figure 5. Regulation of mitochondrial function by MFN2

(A) The effects of MFN2 on mitochondrial abundance and ROS were detected by MitoTracker and MitoSOX fluorescence staining and (B) colocalization analysis.

(B) Seahorse bioanalyzer was used to detect the effect of MFN2 on mitochondrial respiration induced by Ang II.

(C) Basal respiration, (E) maximum respiration, (F) ATP production, and (G) spare respiration capacity in HUVECs after *siMFN2* or *ovMFN2*. In (B-G), each bar represents the mean ± SD for triplicate experiments (**$p < 0.01$, ***$p < 0.001$; #$p < 0.05$, ##$p < 0.01$, ###$p < 0.001$).

Suppress the activation of p-STAT3 reversed AngII-induced endothelial cell senescence. (Figures 10D and 10E). Then, we verified whether STAT3 could directly act on the BCL6 promoter region by dual luciferase reporter gene assay, and the results showed that STAT3 could directly promote the transcription of BCL6 (Figure 10F). These results suggest that AngII stimulation promotes vascular endothelial cell senescence by regulating the STAT3/BCL6/MFN2 pathway.

DISCUSSION

Endothelial cell senescence is a key contributor to vascular aging and the development of cardiovascular diseases.[23] In this study, we investigated the role of MFN2, a mitochondrial fusion protein, in endothelial cell senescence and its potential implications for the aging process.

First, we found that MFN2 expression is significantly decreased in aging mouse aortic tissues and vascular-associated cells, such as endothelial cells. Our results showed that MFN2 expression was first increased and then decreased in the Ang II-induced endothelial cell senescence model, suggesting that the high expression of MFN2 in the early stage may play an important role in antagonizing the occurrence of senescence, while the reduction of MFN2 in the late stage may lead to senescence. This finding is in line with previous studies reporting the downregulation of MFN2 in other cell types associated with aging, including fibroblasts and neurons.[24–26] However, this biphasic response of MFN2 to Ang II stimulation suggests a more complex regulatory mechanism for this gene in endothelial cells.

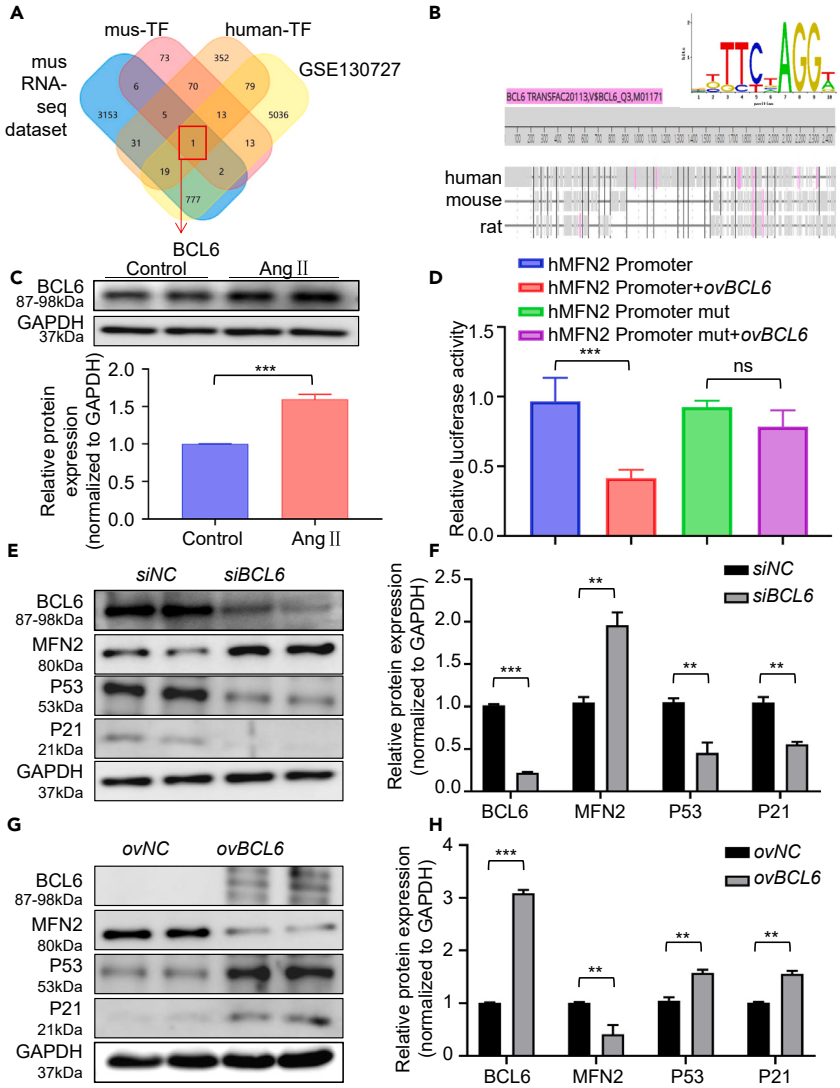

Figure 6. BCL6 is a negatively regulated transcription factor that regulates MFN2

(A) Venn diagram of the four databases.

(B) Predicted binding sites of BCL6 in the MFN2 promoter region.

(C) Expression and quantification of BCL6 in HUVECs stimulated by Ang II. Each bar represents the mean ± SD for triplicate experiments. Mean data are normalized to GAPDH (***$p < 0.001$).

(D) Dual fluorescence reporter gene assay was used to verify that BCL6 inhibited the transcriptional activity of MFN2. Each bar represents the mean ± SD (***$p < 0.001$).

(E) The protein expression and (F) quantification of MFN2, P53, and P21 in HUVECs after *siBCL6*. Each bar represents the mean ± SD for triplicate experiments. Mean data are normalized to GAPDH (**$p < 0.01$, ***$p < 0.001$).

(G) The protein expression and (H) quantification of MFN2, P53, and P21 in HUVECs after *ovBCL6*. Each bar represents the mean ± SD for triplicate experiments. Mean data are normalized to GAPDH (**$p < 0.01$, ***$p < 0.001$).

To further investigate the functional significance of MFN2 in endothelial cell senescence, the expression changes of senescence-related genes in HUVECs after AngII stimulation were analyzed. Our analysis revealed an inverse correlation between MFN2 expression and the expression of senescence-related genes, such as P21 and P53. This observation is consistent with previous studies implicating the dysregulation of these genes in cellular senescence and aging.[27,28]

Recent studies have shown that MFN2 plays important roles in mitochondrial dynamics, DNA damage repair, and apoptosis regulation, all of which are closely related to cellular senescence.[29–31] Therefore, the down-regulation of MFN2 in endothelial cells may contribute to the development of age-related vascular diseases. Functional assays conducted in our study revealed that Ang II-induced endothelial cell senescence was associated with reduced cell proliferation and increased senescence, as evidenced by β-Gal staining and Ki67 immunofluorescence

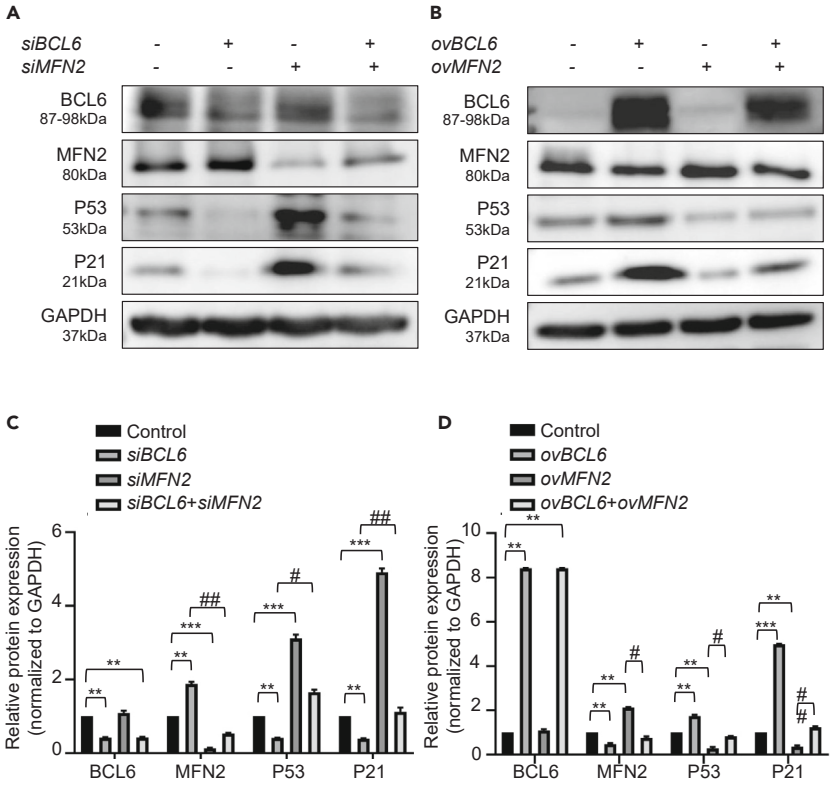

Figure 7. BCL6 regulates endothelial cell senescence through MFN2

(A) Protein expression levels and (C) quantification of P53, P21, and other genes after *siMFN2* and *siBCL6*.

(B) Protein expression levels and (D) quantification of P53, P21, and other genes after *ovMFN2* and *ovBCL6*. In (C and D), each bar represents the mean ± SD for triplicate experiments (**$p < 0.01$, ***$p < 0.001$; #$p < 0.05$, ##$p < 0.01$).

staining. These findings are consistent with previous studies demonstrating the link between MFN2 downregulation and decreased cell proliferation, as well as increased cellular senescence.[16,32] The dysregulation of MFN2 may disrupt mitochondrial dynamics and impair cellular functions, contributing to the progression of endothelial cell senescence.

Our study provides evidence that MFN2 plays a crucial role in regulating Ang II-induced endothelial cell senescence. Through siRNA-mediated knockdown and overexpression experiments, we demonstrated that MFN2 expression changes contribute to the development of endothelial cell aging and that manipulating MFN2 levels can modulate this process.

The downregulation of MFN2 using siRNA resulted in increased endothelial cell senescence, as evidenced by β-Gal staining and reduced cell proliferation. These findings are consistent with previous studies that have linked MFN2 downregulation to cellular senescence in various cell types.[33,34] Furthermore, the *siMFN2*-induced endothelial cell senescence was exacerbated when combined with Ang II stimulation, indicating a synergistic effect between the two factors. On the other hand, *ovMFN2* attenuated Ang II-induced endothelial cell senescence and increased cell proliferation. This observation is in line with previous reports demonstrating the protective effects of MFN2 overexpression against cellular senescence.[35] The ability of MFN2 to modulate cellular senescence may be attributed to its role in regulating mitochondrial fusion and maintaining mitochondrial function, which are critical for cellular homeostasis.

At the protein level, we observed that *siMFN2* treatment led to significant upregulation of senescence-related proteins, including P21 and P53, with an even more pronounced effect in the presence of Ang II. These findings are consistent with previous studies that have implicated P21 and P53 in cellular senescence and aging.[36,37] Conversely, *ovMFN2* attenuated the increase in P21 and P53 induced by Ang II, thereby mitigating cell senescence. This suggests that MFN2 may modulate endothelial cell senescence in part through its effects on these senescence-associated proteins.

Our study provides mechanistic insights into the role of MFN2 in cellular senescence by examining its effects on mitochondrial morphology and function. Mitochondria, as key regulators of cellular homeostasis, have been implicated in the process of cellular senescence.[38] In this study, we observed that the depletion of MFN2 resulted in mitochondrial fragmentation and increased production of reactive oxygen species (ROS) in endothelial cells, consistent with previous studies linking MFN2 to mitochondrial morphology and function.

Mitochondrial fragmentation, characterized by smaller and fragmented mitochondria, has been associated with impaired mitochondrial function and increased cellular senescence.[39,40] Our findings demonstrate that the downregulation of MFN2 exacerbates mitochondrial morphological damage and ROS production induced by Ang II stimulation, indicating a synergistic effect between MFN2 depletion and

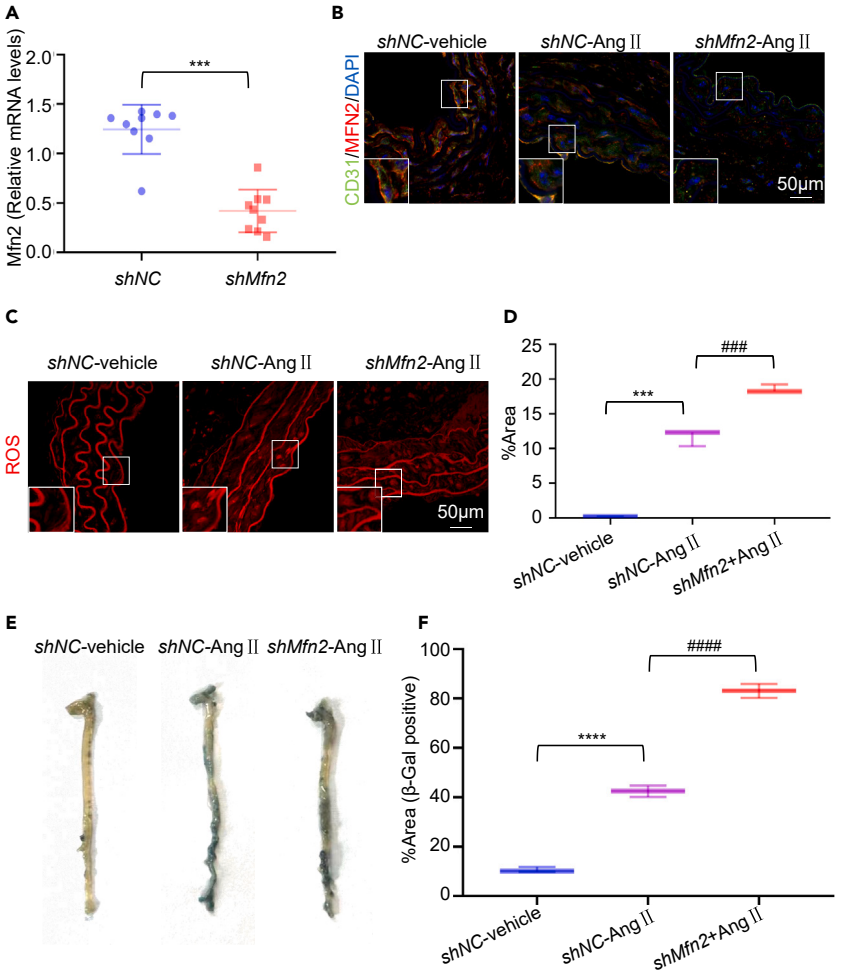

Figure 8. AAV-*shMfn2* aggravated Ang II-induced vascular senescence in ApoE$^{-/-}$ mice

(A) Mfn2 mRNA level expression in mouse aorta. Each bar represents the mean ± SD (n = 9). Mean data are normalized to 18s.

(B) Immunofluorescence co-staining of MFN2/CD31 in mouse aorta.

(C) ROS staining and (D) quantification of mouse aorta.

(D) β-GAL staining and (F) quantification of mouse aorta. In (D and F), each bar represents the mean ± SD for triplicate experiments. (***$p < 0.001$, ****$p < 0.0001$; ###$p < 0.001$, ####$p < 0.0001$).

Ang II on mitochondrial dysfunction and cellular senescence. This is consistent with previous studies that have shown the involvement of MFN2 in maintaining mitochondrial fusion and preventing mitochondrial fragmentation.[41,42]

ROS, byproducts of mitochondrial respiration, play a dual role in cellular senescence, acting as signaling molecules at low levels but causing oxidative damage at high levels.[43,44] Our results revealed that MFN2 depletion resulted in increased ROS production in endothelial cells, further supporting the notion that MFN2 plays a critical role in maintaining mitochondrial function and redox homeostasis. This is in line with previous studies demonstrating the association between MFN2 and ROS production in various cellular contexts.[45,46]

Furthermore, we investigated the functional consequences of MFN2 depletion on mitochondrial respiration. Our data showed that *siMFN2* and Ang II stimulation significantly reduced the basal respiration, maximal respiration, ATP production, and spare respiratory capacity of mitochondria in endothelial cells. These findings are consistent with studies implicating MFN2 in the regulation of mitochondrial bioenergetics.[47] Importantly, we observed that the detrimental effects on mitochondrial function were exacerbated when MFN2 depletion was combined with Ang II stimulation, suggesting a synergistic effect between MFN2 and Ang II in impairing mitochondrial function and promoting cellular senescence.

BCL6, a transcription factor of the BCL6 corepressor gene family, has been implicated in various biological processes, including cell proliferation, apoptosis, and immune responses.[48,49] However, its role in endothelial cell senescence and mitochondrial function has not been extensively studied. To explore the molecular mechanism of senescence-related reduction of MFN2 expression, transcription factors in the MFN2 promoter region were predicted and intersected with the differentially expressed genes in GSE130727 dataset and mouse vascular tissue. We identified BCL6 as a potential transcription factor upstream of MFN2, and our results suggest that Ang II regulates endothelial

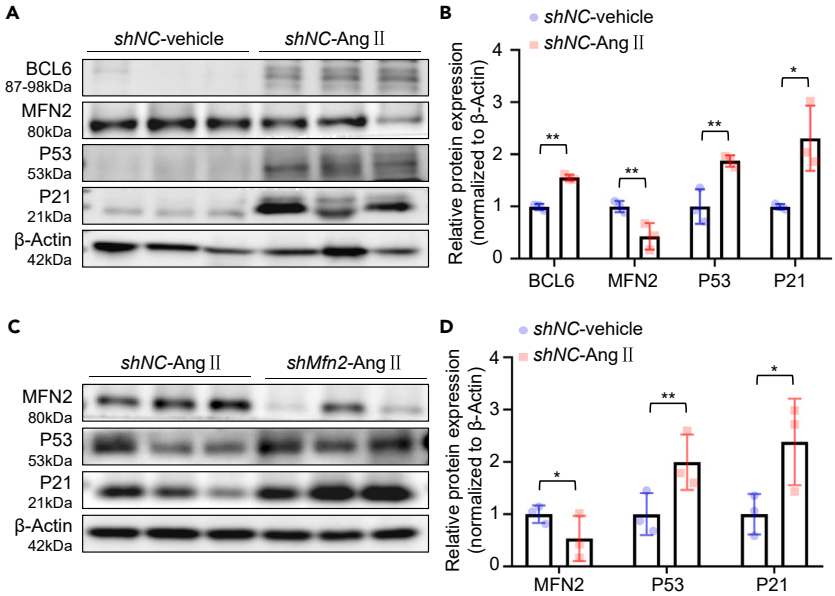

Figure 9. Knock-down of MFN2 in ApoE$^{-/-}$ mice aggravated vascular senescence by affecting the expression of P53 and P21

(A) To investigate the effect of Ang II stimulation on the expression of BCL6, MFN2, P53, and P21 proteins in mice aorta and (B) quantification.

(B) Effects of *shMfn2* followed by Ang II stimulation on MFN2, P53, and P21 protein expression in mice aorta and (D) quantification. In (B and D), each bar represents the mean ± SD ($n = 3$). Mean data are normalized to β-Actin. (*$p < 0.05$, **$p < 0.01$).

cell senescence by increasing the expression of BCL6. This suggests that the BCL6/MFN2 axis is involved in modulating mitochondrial dynamics and promoting endothelial cell senescence. Our study provides insights into the involvement of BCL6 in regulating MFN2 expression and cellular senescence in the context of Ang II stimulation.

In our *in vivo* experiments, we utilized AAV-*shMfn2* adeno-associated virus to knockdown MFN2 expression in ApoE$^{-/-}$ mice. Subcutaneous sustained release of Ang II was then administered to induce endothelial cell senescence. Our results demonstrated that MFN2 deficiency significantly aggravated Ang II-induced vascular endothelial cell senescence. These findings suggest that MFN2 may play a protective role in maintaining endothelial cell function and preventing senescence.

BCL6 was found to play a role in Ang II-induced endothelial senescence by negatively regulating MFN2 expression. We investigated the expression levels of BCL6, P21, and P53 in vascular tissues. Our results demonstrated that the expressions of BCL6, P21, and P53 were up-regulated in the vascular tissues of Ang II-treated mice. Importantly, loss of BCL6 further enhanced the down-regulation of P21 and P53 expression, suggesting that BCL6/MFN2 signaling pathway can regulate endothelial cell senescence.

Our study suggests that MFN2 plays a protective role in maintaining endothelial cell function and preventing senescence. The dysregulation of MFN2 disrupts mitochondrial dynamics, impairs mitochondrial function, and exacerbates cellular senescence. Restoring MFN2 expression or enhancing its activity may hold promise as a therapeutic strategy to alleviate endothelial dysfunction and delay the progression of vascular aging.

Overall, our study highlights the importance of MFN2 in regulating endothelial cell senescence and provides mechanistic insights into the role of MFN2 in maintaining endothelial cell homeostasis.

Limitations of the study

We found that Ang II stimulation promoted vascular endothelial cell senescence through the STAT3/BCL6/MFN2 pathway, and the knock-down of Mfn2 *in vivo* indeed promoted vascular senescence in mice. However, the lack of this research lies in 1) lack of specificity on low or overexpression of Mfn2 *in vivo* experiments to verify the endothelial cells specificity Mfn2 express missing or increase of Ang II vascular tissue, the effect of aging mice induced by this will be our next plan; 2) The mechanism by which MFN2 depletion in endothelial cells promotes vascular senescence is still unclear, and we plan to generate endothelium-specific Mfn2 knockout mice to further explore this mechanism.

RESOURCE AVAILABILITY

Lead contact

Further information and requests for resources should be directed to and will be fulfilled by the lead contact, Xiaozeng Wang (wxiaozeng@163.com).

Materials availability

This study did not generate new unique reagents.

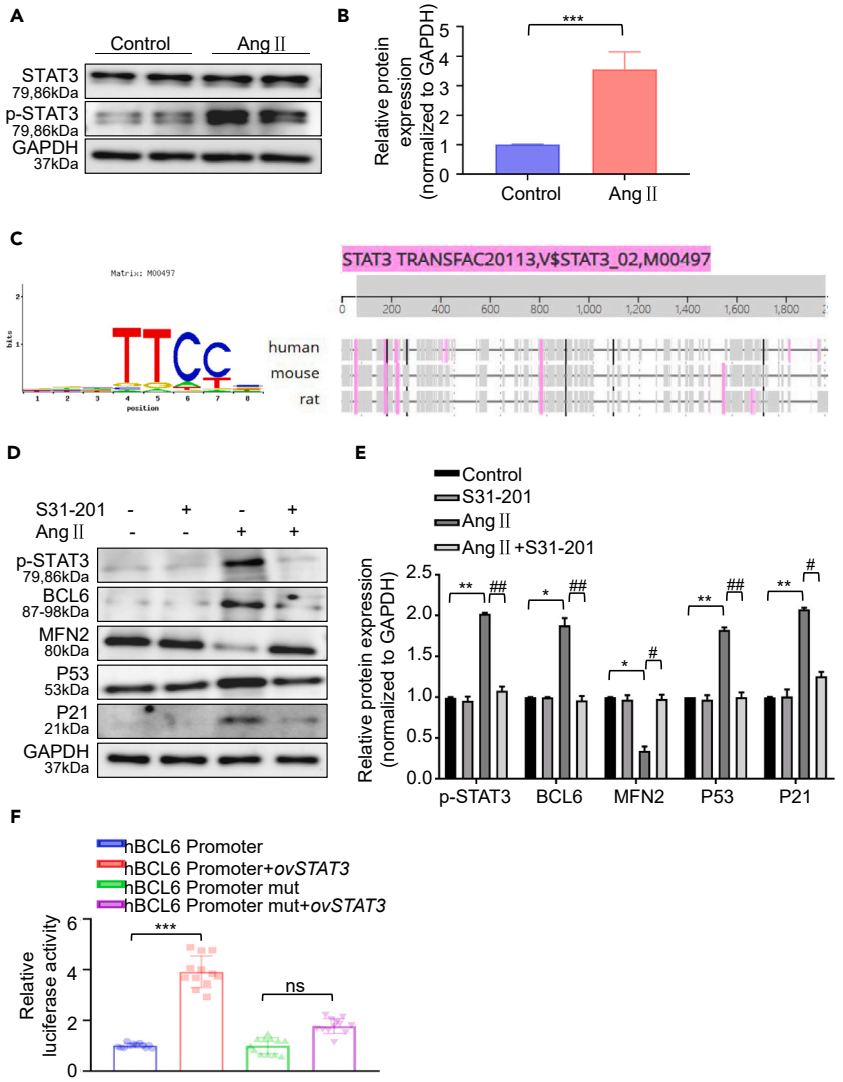

Figure 10. Ang II stimulating the increase of STAT3 phosphorylation promotes BCL6 expression in Ang II-induced cell aging

(A) Expression and quantification (B) of p-STAT3 in HUVECs stimulated by Ang II.

(C) STAT3 site prediction combined with BCL6 promoter region.

(D) The protein expression levels and (E) their quantification of BCL6, MFN2, P53, and P21 in HUVECs were assessed following treatment with p-STAT3 inhibitors (S31-201) and stimulation with Ang II.

(F) Dual luciferase reporter assay confirmed that STAT3 promoted the transcriptional activity of BCL6. Each bar represents the mean ± SD. (***$p < 0.001$). In (B and E), each bar represents the mean ± SD for triplicate experiments. (*$p < 0.05$, **$p < 0.01$, ***$p < 0.001$; #$p < 0.05$, ##$p < 0.01$).

Data and code availability

- This article analyzes existing, publicly available data. These accession numbers for the datasets are listed in the key resources table.
- This article does not report original code.
- Original western blot images have been deposited at Mendeley (https://doi.org/10.17632/yjy483tdz7.1) and are publicly available as of the date of publication. Any additional information required to reanalyze the data reported in this article is available from the lead contact upon request.

ACKNOWLEDGMENTS

We thank GEO database for providing their platforms. We are grateful to all the researchers involved in this study. The study was supported by the Applied Basic Research Program of Liaoning Province (2022JH2/101300054), Liaoning Provincial Natural Science Foundation (2022-BS-035), National Natural Science Foundation of China (82270449) and National Key Research and Development Program of China (grant no. 2020-YFC-2008100, 2022-YFC-2503403).

AUTHOR CONTRIBUTIONS

Jiayin Li: Methodology, software and formal analysis, and writing - original draft; Zheming Yang and Jing Liu: writing - review and editing and formal analysis; Haixu Song: writing - review and editing; Lin Yang: conceptualization: Kun Na: formal analysis; Zhu Mei: formal analysis; Shuli Zhang: methodology; Chenghui Yan: conceptualization, methodology, writing - review and editing, and supervision; Xiaozeng Wang: conceptualization, methodology, writing - review and editing, and supervision. All authors have read and agreed to the published version of the article.

DECLARATION OF INTERESTS

The authors declare no competing interests.

STAR★METHODS

Detailed methods are provided in the online version of this paper and include the following:

- KEY RESOURCES TABLE
- EXPERIMENTAL MODEL AND STUDY PARTICIPANT DETAILS
  - Cell lines
  - Animals
- METHOD DETAILS
  - Plasmid transfection
  - Microarray analysis of mouse aortic tissue
  - Selection of databases and analysis of differentially expressed genes (DEGs)
  - Weighed gene co-expression network analysis
  - Histology
  - Beta-galactosidase staining
  - Western blot analysis
  - Measurement of mitochondrial abundance and reactive oxygen species
  - Mitochondrial respiration with Seahorse bioanalyzer
  - Construction of plasmids
  - Dual-luciferase reporter gene assay
- QUANTIFICATION AND STATISTICAL ANALYSIS

SUPPLEMENTAL INFORMATION

Supplemental information can be found online at https://doi.org/10.1016/j.isci.2024.110809.

Received: February 29, 2024
Revised: June 18, 2024
Accepted: August 21, 2024
Published: August 24, 2024

REFERENCES

1. Childs, B.G., Durik, M., Baker, D.J., and van Deursen, J.M. (2015). Cellular senescence in aging and age-related disease: from mechanisms to therapy. Nat. Med. *21*, 1424–1435. https://doi.org/10.1038/nm.4000.
2. Gorbunova, V., Seluanov, A., Mita, P., McKerrow, W., Fenyö, D., Boeke, J.D., Linker, S.B., Gage, F.H., Kreiling, J.A., Petrashen, A.P., et al. (2021). The role of retrotransposable elements in ageing and age-associated diseases. Nature *596*, 43–53. https://doi.org/10.1038/s41586-021-03542-y.
3. Liberski, S., Wichrowska, M., and Kocięcki, J. (2022). Aflibercept versus Faricimab in the Treatment of Neovascular Age-Related Macular Degeneration and Diabetic Macular Edema: A Review. Int. J. Mol. Sci. *23*, 9424. https://doi.org/10.3390/ijms23169424.
4. Ungvari, Z., Tarantini, S., Donato, A.J., Galvan, V., and Csiszar, A. (2018). Mechanisms of Vascular Aging. Circ. Res. *123*, 849–867. https://doi.org/10.1161/CIRCRESAHA.118.311378.
5. Jia, G., Aroor, A.R., Jia, C., and Sowers, J.R. (2019). Endothelial cell senescence in aging-related vascular dysfunction. Biochim. Biophys. Acta, Mol. Basis Dis. *1865*, 1802–1809. https://doi.org/10.1016/j.bbadis.2018.08.008.
6. Park, H.S., and Kim, S.Y. (2021). Endothelial cell senescence: A machine learning-based meta-analysis of transcriptomic studies. Ageing Res. Rev. *65*, 101213. https://doi.org/10.1016/j.arr.2020.101213.
7. Bloom, S.I., Islam, M.T., Lesniewski, L.A., and Donato, A.J. (2023). Mechanisms and consequences of endothelial cell senescence. Nat. Rev. Cardiol. *20*, 38–51. https://doi.org/10.1038/s41569-022-00739-0.
8. Hwang, H.J., Kim, N., Herman, A.B., Gorospe, M., and Lee, J.S. (2022). Factors and Pathways Modulating Endothelial Cell Senescence in Vascular Aging. Int. J. Mol. Sci. *23*, 10135. https://doi.org/10.3390/ijms231710135.
9. Zou, M.H., and Wu, S. (2021). Adenosine Monophosphate-Activated Protein Kinase, Oxidative Stress, and Diabetic Endothelial Dysfunction. Cardiol. Discov. *1*, 44–57. https://doi.org/10.1097/CD9.0000000000000009.
10. Sun, D., Chen, S., Li, S., Wang, N., Zhang, S., Xu, L., Zhu, S., Li, H., Gu, Q., Xu, X., and Wei, F. (2023). Enhancement of glycolysis-dependent DNA repair regulated by FOXO1 knockdown via PFKFB3 attenuates hyperglycemia-induced endothelial oxidative stress injury. Redox Biol. *59*, 102589. https://doi.org/10.1016/j.redox.2022.102589.
11. Casella, G., Munk, R., Kim, K.M., Piao, Y., De, S., Abdelmohsen, K., and Gorospe, M. (2019). Transcriptome signature of cellular senescence. Nucleic Acids Res. *47*, 11476–17305. https://doi.org/10.1093/nar/gkz879.
12. Li, X., Straub, J., Medeiros, T.C., Mehra, C., den Brave, F., Peker, E., Atanassov, I., Stillger, K., Michaelis, J.B., Burbridge, E., et al. (2022). Mitochondria shed their outer membrane in response to infection-induced stress. Science *375*, eabi4343. https://doi.org/10.1126/science.abi4343.
13. Hong, Y., He, H., Jiang, G., Zhang, H., Tao, W., Ding, Y., Yuan, D., Liu, J., Fan, H., Lin, F., et al. (2020). miR-155-5p inhibition rejuvenates aged mesenchymal stem cells and enhances cardioprotection following infarction. Aging Cell *19*, e13128. https://doi.org/10.1111/acel.13128.
14. Chen, Y., and Dorn, G.W., 2nd (2013). PINK1-phosphorylated mitofusin 2 is a Parkin receptor for culling damaged mitochondria. Science *340*, 471–475. https://doi.org/10.1126/science.1231031.
15. Chen, L., Liu, B., Qin, Y., Li, A., Gao, M., Liu, H., and Gong, G. (2021). Mitochondrial Fusion Protein Mfn2 and Its Role in Heart Failure. Front. Mol. Biosci. *8*, 681237. https://doi.org/10.3389/fmolb.2021.681237.
16. Zhu, J., Yang, Q., Li, H., Wang, Y., Jiang, Y., Wang, H., Cong, L., Xu, J., Shen, Z., Chen, W., et al. (2022). Sirt3 deficiency accelerates ovarian senescence without affecting

spermatogenesis in aging mice. Free Radic. Biol. Med. *193*, 511–525. https://doi.org/10.1016/j.freeradbiomed.2022.10.324.
17. Nivison, M.P., Ericson, N.G., Green, V.M., Bielas, J.H., Campbell, J.S., and Horner, P.J. (2017). Age-related accumulation of phosphorylated mitofusin 2 protein in retinal ganglion cells correlates with glaucoma progression. Exp. Neurol. *296*, 49–61. https://doi.org/10.1016/j.expneurol.2017.07.001.
18. Cheon, Y., Yoon, S., Lee, J.H., Kim, K., Kim, H.J., Hong, S.W., Yun, Y.R., Shim, J., Kim, S.H., Lu, B., et al. (2023). A Novel Interaction between MFN2/Marf and MARK4/PAR-1 Is Implicated in Synaptic Defects and Mitochondrial Dysfunction. eNeuro *10*. ENEURO.0409-0422.2023. https://doi.org/10.1523/ENEURO.0409-22.2023.
19. Miller, A.J., and Arnold, A.C. (2022). The renin-angiotensin system and cardiovascular autonomic control in aging. Peptides *150*, 170733. https://doi.org/10.1016/j.peptides.2021.170733.
20. Zou, F., Li, Y., Zhang, S., and Zhang, J. (2022). DP1 (Prostaglandin D(2) Receptor 1) Activation Protects Against Vascular Remodeling and Vascular Smooth Muscle Cell Transition to Myofibroblasts in Angiotensin II-Induced Hypertension in Mice. Hypertension *79*, 1203–1215. https://doi.org/10.1161/HYPERTENSIONAHA.121.17584.
21. Montezano, A.C., Nguyen Dinh Cat, A., Rios, F.J., and Touyz, R.M. (2014). Angiotensin II and vascular injury. Curr. Hypertens. Rep. *16*, 431. https://doi.org/10.1007/s11906-014-0431-2.
22. Min, L.J., Mogi, M., Iwai, M., and Horiuchi, M. (2009). Signaling mechanisms of angiotensin II in regulating vascular senescence. Ageing Res. Rev. *8*, 113–121. https://doi.org/10.1016/j.arr.2008.12.002.
23. Incalza, M.A., D'Oria, R., Natalicchio, A., Perrini, S., Laviola, L., and Giorgino, F. (2018). Oxidative stress and reactive oxygen species in endothelial dysfunction associated with cardiovascular and metabolic diseases. Vascul. Pharmacol. *100*, 1–19. https://doi.org/10.1016/j.vph.2017.05.005.
24. Chevrollier, A., Cassereau, J., Ferré, M., Alban, J., Desquiret-Dumas, V., Gueguen, N., Amati-Bonneau, P., Procaccio, V., Bonneau, D., and Reynier, P. (2012). Standardized mitochondrial analysis gives new insights into mitochondrial dynamics and OPA1 function. Int. J. Biochem. Cell Biol. *44*, 980–988. https://doi.org/10.1016/j.biocel.2012.03.006.
25. Cho, D.H., Nakamura, T., and Lipton, S.A. (2010). Mitochondrial dynamics in cell death and neurodegeneration. Cell. Mol. Life Sci. *67*, 3435–3447. https://doi.org/10.1007/s00018-010-0435-2.
26. Han, S., Nandy, P., Austria, Q., Siedlak, S.L., Torres, S., Fujioka, H., Wang, W., and Zhu, X. (2020). Mfn2 Ablation in the Adult Mouse Hippocampus and Cortex Causes Neuronal Death. Cells *9*, 116. https://doi.org/10.3390/cells9010116.
27. Duan, J.L., Ruan, B., Song, P., Fang, Z.Q., Yue, Z.S., Liu, J.J., Dou, G.R., Han, H., and Wang, L. (2022). Shear stress-induced cellular senescence blunts liver regeneration through Notch-sirtuin 1-P21/P16 axis. Hepatology *75*, 584–599. https://doi.org/10.1002/hep.32209.
28. Peng, Y., Du, J., Günther, S., Guo, X., Wang, S., Schneider, A., Zhu, L., and Braun, T. (2022). Mechano-signaling via Piezo1 prevents activation and p53-mediated senescence of muscle stem cells. Redox Biol. *52*, 102309. https://doi.org/10.1016/j.redox.2022.102309.
29. Basha, E.H., Eltokhy, A.K.B., Eltantawy, A.F., Heabah, N.A.E., Elshwaikh, S.L., and El-Harty, Y.M. (2022). Linking mitochondrial dynamics and fertility: promoting fertility by phoenixin through modulation of ovarian expression of GnRH receptor and mitochondrial dynamics proteins DRP-1 and Mfn-2. Pflügers Archiv *474*, 1107–1119. https://doi.org/10.1007/s00424-022-02739-y.
30. Oanh, N.T.K., Lee, H.S., Kim, Y.H., Min, S., Park, Y.J., Heo, J., Park, Y.Y., Lim, W.C., and Cho, H. (2022). Regulation of nuclear DNA damage response by mitochondrial morphofunctional pathway. Nucleic Acids Res. *50*, 9247–9259. https://doi.org/10.1093/nar/gkac690.
31. Shi, J., Yu, J., Zhang, Y., Wu, L., Dong, S., Wu, L., Wu, L., Du, S., Zhang, Y., and Ma, D. (2019). PI3K/Akt pathway-mediated HO-1 induction regulates mitochondrial quality control and attenuates endotoxin-induced acute lung injury. Lab. Invest. *99*, 1795–1809. https://doi.org/10.1038/s41374-019-0286-x.
32. Feng, S., Gao, L., Zhang, D., Tian, X., Kong, L., Shi, H., Wu, L., Huang, Z., Du, B., Liang, C., et al. (2019). MiR-93 regulates vascular smooth muscle cell proliferation, and neointimal formation through targeting Mfn2. Int. J. Biol. Sci. *15*, 2615–2626. https://doi.org/10.7150/ijbs.36995.
33. Xu, T.T., Li, H., Dai, Z., Lau, G.K., Li, B.Y., Zhu, W.L., Liu, X.Q., Liu, H.F., Cai, W.W., Huang, S.Q., et al. (2020). Spermidine and spermine delay brain aging by inducing autophagy in SAMP8 mice. Aging *12*, 6401–6414. https://doi.org/10.18632/aging.103035.
34. Vezza, T., Díaz-Pozo, P., Canet, F., de Marañón, A.M., Abad-Jiménez, Z., García-Gargallo, C., Roldan, I., Solá, E., Bañuls, C., López-Domènech, S., et al. (2022). The Role of Mitochondrial Dynamic Dysfunction in Age-Associated Type 2 Diabetes. World J. Mens Health *40*, 399–411. https://doi.org/10.5534/wjmh.210146.
35. Escobar-Henriques, M., and Joaquim, M. (2019). Mitofusins: Disease Gatekeepers and Hubs in Mitochondrial Quality Control by E3 Ligases. Front. Physiol. *10*, 517. https://doi.org/10.3389/fphys.2019.00517.
36. Al-Dabet, M.M., Shahzad, K., Elwakiel, A., Sulaj, A., Kopf, S., Bock, F., Gadi, I., Zimmermann, S., Rana, R., Krishnan, S., et al. (2022). Reversal of the renal hyperglycemic memory in diabetic kidney disease by targeting sustained tubular p21 expression. Nat. Commun. *13*, 5062. https://doi.org/10.1038/s41467-022-32477-9.
37. Sha, J.Y., Li, J.H., Zhou, Y.D., Yang, J.Y., Liu, W., Jiang, S., Wang, Y.P., Zhang, R., Di, P., and Li, W. (2021). The p53/p21/p16 and PI3K/Akt signaling pathways are involved in the ameliorative effects of maltol on D-galactose-induced liver and kidney aging and injury. Phytother Res. *35*, 4411–4424. https://doi.org/10.1002/ptr.7142.
38. Dhillon, R.S., and Denu, J.M. (2017). Using comparative biology to understand how aging affects mitochondrial metabolism. Mol. Cell. Endocrinol. *455*, 54–61. https://doi.org/10.1016/j.mce.2016.12.020.
39. Ahola, S., Rivera Mejías, P., Hermans, S., Chandragiri, S., Giavalisco, P., Nolte, H., and Langer, T. (2022). OMA1-mediated integrated stress response protects against ferroptosis in mitochondrial cardiomyopathy. Cell Metabol. *34*, 1875–1891.e7. https://doi.org/10.1016/j.cmet.2022.08.017.
40. Liesa, M., and Shirihai, O.S. (2013). Mitochondrial dynamics in the regulation of nutrient utilization and energy expenditure. Cell Metabol. *17*, 491–506. https://doi.org/10.1016/j.cmet.2013.03.002.
41. Rocha, A.G., Franco, A., Krezel, A.M., Rumsey, J.M., Alberti, J.M., Knight, W.C., Biris, N., Zacharioudakis, E., Janetka, J.W., Baloh, R.H., et al. (2018). MFN2 agonists reverse mitochondrial defects in preclinical models of Charcot-Marie-Tooth disease type 2A. Science *360*, 336–341. https://doi.org/10.1126/science.aao1785.
42. Lozhkin, A., Vendrov, A.E., Ramos-Mondragón, R., Canugovi, C., Stevenson, M.D., Herron, T.J., Hummel, S.L., Figueroa, C.A., Bowles, D.E., Isom, L.L., et al. (2022). Mitochondrial oxidative stress contributes to diastolic dysfunction through impaired mitochondrial dynamics. Redox Biol. *57*, 102474. https://doi.org/10.1016/j.redox.2022.102474.
43. Guo, Y., Guan, T., Shafiq, K., Yu, Q., Jiao, X., Na, D., Li, M., Zhang, G., and Kong, J. (2023). Mitochondrial dysfunction in aging. Ageing Res. Rev. *88*, 101955. https://doi.org/10.1016/j.arr.2023.101955.
44. Nakamura, T., Naguro, I., and Ichijo, H. (2019). Iron homeostasis and iron-regulated ROS in cell death, senescence and human diseases. Biochim. Biophys. Acta Gen. Subj. *1863*, 1398–1409. https://doi.org/10.1016/j.bbagen.2019.06.010.
45. Jiang, Y., Krantz, S., Qin, X., Li, S., Gunasekara, H., Kim, Y.M., Zimnicka, A., Bae, M., Ma, K., Toth, P.T., et al. (2022). Caveolin-1 controls mitochondrial damage and ROS production by regulating fission - fusion dynamics and mitophagy. Redox Biol. *52*, 102304. https://doi.org/10.1016/j.redox.2022.102304.
46. Tur, J., Pereira-Lopes, S., Vico, T., Marín, E.A., Muñoz, J.P., Hernández-Alvarez, M., Cardona, P.J., Zorzano, A., Lloberas, J., and Celada, A. (2020). Mitofusin 2 in Macrophages Links Mitochondrial ROS Production, Cytokine Release, Phagocytosis, Autophagy, and Bactericidal Activity. Cell Rep. *32*, 108079. https://doi.org/10.1016/j.celrep.2020.108079.
47. Kawalec, M., Boratyńska-Jasińska, A., Beręsewicz, M., Dymkowska, D., Zabłocki, K., and Zabłocka, B. (2015). Mitofusin 2 Deficiency Affects Energy Metabolism and Mitochondrial Biogenesis in MEF Cells. PLoS One *10*, e0134162. https://doi.org/10.1371/journal.pone.0134162.
48. Louwen, F., Kreis, N.N., Ritter, A., Friemel, A., Solbach, C., and Yuan, J. (2022). BCL6, a key oncogene, in the placenta, pre-eclampsia and endometriosis. Hum. Reprod. Update *28*, 890–909. https://doi.org/10.1093/humupd/dmac027.
49. Chen, Z., Wang, W., and Hua, Y. (2023). Identification and validation of BCL6 and VEGFA as biomarkers and ageing patterns correlating with immune infiltrates in OA progression. Sci. Rep. *13*, 2558. https://doi.org/10.1038/s41598-023-28000-9.
50. Langfelder, P., and Horvath, S. (2008). WGCNA: an R package for weighted correlation network analysis. BMC Bioinf. *9*, 559. https://doi.org/10.1186/1471-2105-9-559.

STAR★METHODS

KEY RESOURCES TABLE

REAGENT or RESOURCE	SOURCE	IDENTIFIER
Antibodies		
anti-MFN2	Cell Signaling Technology	Cat# 9482S; RRID: AB_2818867
anti-P21	Santa Cruz	Cat# sc-6246; RRID: AB_2315147
anti-P53	Abclonal	Cat# A0263; RRID: AB_2736796
anti-BCL6	Cell Signaling Technology	Cat# 14895S; RRID: AB_2798638
anti-β-Actin	Santa Cruz	Cat# sc-47778; RRID: AB_627675
anti-GAPDH	Cell Signaling Technology	Cat# 2118S; RRID: AB_2315148
Bacterial and virus strains		
AAV-shMfn2 adeno-associated virus	OBiO Technology	
Chemicals, peptides, and recombinant proteins		
RIPA buffer	Thermo Fisher Scientific	89901
BCA Protein Assay Reagent Kit	Thermo Fisher Scientific	A55860
Lipofectamine 2000	Thermo Fisher Scientific	11668019
Lipofectamine RNAiMAX	Thermo Fisher Scientific	13778150
Prime Script RT reagent kit	Takara	RR037A
Angiotensin II	ApexBio Technology	A1042
β-Gal staining kit	Solarbio	G1580
MitoTracker Green	Thermo Fisher Scientific	M7514
MitoSOX Red	Thermo Fisher Scientific	M36008
Deposited data		
HUCPVC dataset	Gene Expression Omnibus	GSE119987
Mouse Aortic dataset	Gene Expression Omnibus	GSE198045
HMVWC dataset	Gene Expression Omnibus	GSE230181
HUVEC dataset	Gene Expression Omnibus	GSE130727
Original western blot images	Mendeley	https://doi.org/10.17632/yjy483tdz7.1
Experimental models: Cell lines		
HUVECs	the Cell Bank at the Chinese Academy of Sciences	
Experimental models: Organisms/strains		
Mouse: ApoE$^{-/-}$	Nanjing Model Animal Center	
Oligonucleotides		
Primer h-MFN2 forward: CTCTCGATGCAACTCTATCGTC	Sangon Biotech	
Primer h-MFN2 reverse: TCCTGTACGTGTCTTCAAGGAA	Sangon Biotech	
Primer *m*-MFN2 forward: ACCCCGTTACCACAGAAGAAC	Sangon Biotech	
Primer *m*-MFN2 reverse: AAAGCCACTTTCATGTGCCTC	Sangon Biotech	
Primer h-BCL6 forward: ACACATCTCGGCTCAATTTGC	Sangon Biotech	

(*Continued on next page*)

Continued

REAGENT or RESOURCE	SOURCE	IDENTIFIER
Primer h-BCL6 reverse: AGTGTCCACAACATGCTCCAT	Sangon Biotech	
Recombinant DNA		
Plasmid: pcDNA3.1-MFN2	Genewiz	
Plasmid: pGL3-MFN2-promoter	Genewiz	
Plasmid: pGL3-MFN2-promoter-mut	Genewiz	
Plasmid: pcDNA3.1-BCL6	Genewiz	
Plasmid: pGL3-BCL6-promoter	Genewiz	
Plasmid: pGL3-BCL6-promoter-mut	Genewiz	
Software and algorithms		
R	R core	https://www.r-project.org/
ImageJ	National Institutes of Health	https://imagej.nih.gov/ij/
GraphPad Prism version 8.0.1	Bio-Rad Laboratories	https://chameleonimagelab.com/
Image Pro Plus	Image Pro PlusMedia Cybernetics	https://mediacy.com/products/image-pro-plus/

EXPERIMENTAL MODEL AND STUDY PARTICIPANT DETAILS

Cell lines

The human umbilical vein endothelial cells (HUVECs), was acquired from the Cell Bank at the Chinese Academy of Sciences. HUVECs were grown in Endothelial Cell Medium (Life Technologies Corporation, Carlsbad, CA, USA) and other cells were grown in Dulbecco's modified Eagle's medium (Life Technologies Corporation, Carlsbad, CA, USA) containing 10% fetal bovine serum, and cells used for experiments were controlled to within 15 passages.

Animals

Seven-week-old male ApoE$^{-/-}$ mice were bought from the Nanjing Model Animal Center (Nanjing, China). The mice were separated randomly into three groups (n = 15). Two groups of mice was injected with *AAV-shNC* adeno-associated virus, and the other group was injected with *AAV-shMfn2* adeno-associated virus (OBiO Technology, Shanghai). Three weeks later, one group of *AAV-shNC*-mice and *AAV-shMfn2-mice* were given subcutaneous sustained release of Ang II (ApexBio Technology, USA, 1.44 mg/kg/d) by a subcutaneous sustained release pump for 28 days. The remaining group performed vehicle embedding pump. All animal experiments were complied with Directive 2010/63/EU, Commission Implementing Decision (EU) 2020/569, Recommendation 2007/526/EC and 1991 International Guidelines for Ethical Review of Epidemiological Studies.

METHOD DETAILS

Plasmid transfection

Lipofectamine RNAiMAX (Invitrogen, Fisher Scientific, NY) reagent was used to transfect MFN2 small interfering RNA (*siMFN2*, 100 nM) (Ribobio, Guangzhou, China) into HUVECs. Then, using Lipofectamine 2000 reagent (Invitrogen, Fisher Scientific, NY), 400 ng of pcDNA3.1-MFN2 (*ovMFN2*) constructs (Figure S2A) were transfected into HUVECs. HUVECs were stimulated with 10 μM Ang II, After 36 h, the cells were harvested.

Microarray analysis of mouse aortic tissue

Mice aorta RNA microarray analysis was performed on the vascular tissues of ApoE$^{-/-}$ mice and mice treated with 28 days of AngII release pump (n = 3). Total RNA was quantified by the NanoDrop ND-2000 (Thermo Fisher Scientific, USA) and the RNA integrity (RIN) was assessed using Agilent Bioanalyzer 2100 (Agilent, CA). The sample labeling, microarray hybridization and washing were performed based on the manufacturer's standard protocols. Briefly, total RNA were dephosphorylated, denaturated and then labeled with Cyanine-3-CTP. After purification the labeled RNAs were hybridized onto the microarray. After washing, the arrays were scanned with the Agilent Scanner G2505C (Agilent, CA). Feature Extraction software (version10.7.1.1, Agilent, CA) was used to analyze array images to get raw data. Next, Genespring software (version 14.8, Agilent, CA) was employed to finish the basic analysis with the raw data.

Selection of databases and analysis of differentially expressed genes (DEGs)

From the GEO database, four microarray gene expression datasets (GSE119987, GSE198045, GSE230181 and GSE130727) pertaining to cell senescence were chosen. Aliquots of 1 million cells from 4 donor populations of HUCPVCs were thawed from cryopreservation and subject to independent, continuous *in vitro* culture in serum- and xeno-free media until they reached replicative senescence, the first generation of cells was selected as the Young, and the cells of replication 12 to 16 passages were selected as the Aged for analysis in the GSE119987. The GSE198045 database contains the entire RNA sequencing of aortic tissue from C57BL/6 mice at 2 and 28 months of age, with 5 mice in each group. HMVECs and HUVECs were exposure to ionizing radiation (IR) in the GSE230181 and GSE130727 datasets. DESeq2 (RRID: SCR_015687) and LIMMA (RRID: SCR_010943) were utilised for standardisation and differential analysis, while R Project (RRID: SCR_001905) was used to execute the difference analysis of the mouse microarray data and GSE119987 data. Heatmaps of the DEGs were created by R, with a statistically significant cutoff value of $|\log2(FC)| > 1$ and $p < 0.05$. An independent Student's t-test in GraphPad Prism (version 8.0.1) was used to analyze the difference in MFN2 gene expression between distinct sample groups (Aged vs. Young, IR vs. Control).

Weighed gene co-expression network analysis

WGCNA is a bioinformatics technique for identifying the significant trait-related genes.[50] Co-expression network network of mouse aortic tissue was built in R using the "WGCNA" package (RRID: SCR_003302). Using the excellent SampleGenes approach, we eliminated the abnormally expressed genes from mouse aortic tissue microarray data. To assure the building of a scale-free network, an adequate soft threshold power was established to turn the similarity matrix into an adjacency matrix (power = 9). For each pairwise gene, the spearman's correlation matrices and average linkage approach were used, and the similarity matrix was created by calculating the correlation coefficient between gene pairs. The adjacency was then transformed into a topological overlap matrix (TOM) to measure each gene's mean network connectivity, defined as the sum of its adjacency with all other genes for network generation, and the corresponding dissimilarity (1-TOM) was calculated to form clusters. Co-expressed genes were divided into various gene modules using average linkage hierarchical clustering, which was based on the TOM-based dissimilarity measure with a minimum size of 60 for the genes dendrogram. To further analyze the module, we calculated the dissimilarity of module eigen (ME) genes, chose a cut line for module dendrogram and merged some module. We combined the modules with distance of less than 0.25, and finally obtained 22 co-expression modules shown in different colors, the green module was used to conduct our subsequent analysis.

Histology

Aorta tissues were dried, embedded in paraffin, and sectioned after being fixed in 4% paraformaldehyde for 48 h for histological investigations. Immunofluorescent staining and ROS staining (Beyotime Biotechnology, China) were used to color tissue slices.

Beta-galactosidase staining

Fresh aortic tissues or treated cells were fixed in β-Gal fixative solution at room temperature. After 15 min of fixation, the tissues were washed, and an appropriate amount of prepared β-Gal staining solution (now used and prepared) was added. The next day, tissues or cells were washed and photographed. β-Gal staining solution was purchased from Solebo Inc (Solarbio G1580, Beijing, China). The kit used X-Gal as substrate and produced dark blue products under the catalysis of senescence-specific β-galactosidase. The blue cells and tissues were easily observed under the optical microscope, and the blue β-Gal positive part was quantitatively analyzed.

Western blot analysis

Tissues and cells were homogenized in protease and phosphatase inhibitor-laced RIPA buffer (Thermo Fisher Scientific, USA). The BCA Protein Assay Reagent Kit (Thermo Fisher Scientific, USA) was used to calculate the protein content. Antibodies specific for MFN2 (Cell Signaling Technology, USA, 9482S), P21 (Santa Cruz, USA, sc-6246), P53 (Abclonal, China, A0263), BCL6 (Cell Signaling Technology, USA, 14895S), β-Actin (Santa Cruz, USA, sc-47778) and GAPDH (Cell Signaling Technology, USA, 2118S) were used to detect expression of the corresponding protein in 20 μg total protein. Using the ImageJ analysis software, we were able to determine the band intensity by calculating the mean grayscale value.

Measurement of mitochondrial abundance and reactive oxygen species

Mitochondrial abundance was determined with MitoTracker Green (Invitrogen, Fisher Scientific, NY) and mitochondrial ROS production with MitoSOX Red (Invitrogen, Fisher Scientific, NY). The stock solution of the dyes was prepared which were further diluted for a working concentration according to the manufacturer's recommendation. Cells was incubated with MitoTracker Green at 200 nM concentration and MitoSOX Red at 5 μM concentration. This reaction was carried out in confocal cell culture dishes for fluorescent imaging of live cells counter stained with 4′,6-diamidino-2-phenylindole (DAPI) using a Zeiss LSM800 Airyscan confocal microscope (Carl Zeiss, NY).

Mitochondrial respiration with Seahorse bioanalyzer

Cell Mito Stress Tests was performed using a Seahorse XFe96 Analyzer (Agilent, CA). An equal number of cells (20,000 ASCs/well) were seeded in Seahorse cell culture microplates (Agilent, CA) 1 day prior to the experiment sand incubated in MesenPro growth media at

37°C and5% CO2 overnight. The sensor cartridges were hydrated in Seahorse XF Calibrant Solution (Agilent, CA)overnight and incubated in a non-CO2, 37°C incubator 1 day before the experiment. XF Assay media was prepared according to the manufacturer's instructions containing Agilent Seahorse XF Base Medium, 10.5 mM glucose, 1 mM sodium pyruvate, 2 mM L-glutamine, and 5 mM HEPES, and the pH was adjusted to 7.4. An automated protocol for the Cell Mito Stress Test used serial injections of inhibitors and uncouplers to determine the oxygen consumption rate (OCR) in each respiratory state. After a period of equilibration, the basal OCR was determined. Then, 1.0 μM oligomycin, an ATP synthase inhibitor, was added to determine leak respiration that is not coupled to the ATP synthesis. Afterward, 1.0 μM FCCP was added to determine the maximal respiration of the electron transport chain. Finally, 0.5 μM rotenone/antimycin A was added to inhibit complexes I and II, respectively, to determine the residual respiration indicating proton leak in the mitochondria after inhibition of the electron transport chain.

Construction of plasmids

The B-cell lymphoma 6 (BCL6) CDS region sequence was put into the pcDNA3.1 vector (Figure S2D)(Genewiz, China). The promoter and mutant promoter of MFN2 were introduced into the pGL3-Report (Genewiz, China) plasmid to create dual-luciferase reporter plasmids (Figures S2G and S2H). The plasmid DNA was extracted using DNA endotoxin-free plasmid purification kits (Promega, USA).

Dual-luciferase reporter gene assay

The Dual-Luciferase Reporter Assay System (Promega, USA) was used to measure luciferase activity according to the manufacturer's instructions. To control for transfection efficiency, the reporter gene was a firefly and Renilla Dual-Luciferase system, and Renilla activity was normalized to firefly activity.

QUANTIFICATION AND STATISTICAL ANALYSIS

The results of this experiment are shown as mean ± SD. Student's t-tests were employed for comparisons within groups, and one-way analyses of variance were used for comparisons involving more than two groups. GraphPad Prism version 8.0.1 was used for all statistical analyses. ImageJ and Image Pro Plus were used for image quantification. 0.05 was chosen as the cutoff for statistical significance.